

Shape Optimization of Free-form Shells Considering Strain Energy and Algebraic Invariants of Parametric Surface

Shinnosuke FUJITA*, Makoto OHSAKI^a

*Graduate Student, Dept. of Architecture and Architectural Eng., Kyoto University
Kyotodaigaku-Katsura, Nishikyo-ku, Kyoto 615-8540, Japan
Email : rp2-fujita@archi.kyoto-u.ac.jp

^aAssociate Professor, Dept. of Architecture and Architectural Eng., Kyoto University

Abstract

A new approach is proposed for shape optimization of shell surfaces, where requirements on the aesthetic aspect and the constructability as well as the structural rationality are simultaneously considered in the problem formulation. The surface shape is modeled using Bézier surface to reduce the number of variables, while the ability to generate moderately complex shape is maintained. To apply the new approach to shell structures that have various plan shapes, the surface shape which has a rectangle plan is modeled using a tensor product Bézier surface, and the surface shape with an irregular plan is modeled using a triangular patch Bézier surface. The strain energy is used to represent the mechanical performance, and the aesthetic aspects and smoothness of the surface are quantified by algebraic invariants of the surface. The developable surface that has high constructability is created by imposing appropriate algebraic invariants constraints. The effectiveness of the present approach is confirmed through several numerical examples and the characteristics of the results are discussed.

Keywords: shape optimization, nonlinear programming, sensitivity analysis, Bézier surface, algebraic invariants.

1. Introduction

Advancement of computer technologies as well as the developments of structural materials and construction methods enabled us to design so called *free-form shell*, which has complex shape and topology that cannot be categorized to traditional shapes. However, the mechanical behavior of such shell is very complicated, and it is very difficult for a designer to decide feasible shape of a real-world structure based on his/her experience and intuition as a compromise of aesthetical property and mechanical rationality. Furthermore, it is important in practical design that the smoothness of the shape should be maintained while moderately complex geometry is searched. It may be possible for the designer to assign the most desired

shape explicitly. However, in some cases some local and global properties can be assigned for the target shape. In this respect, qualitative measures for defining roundness may be effectively utilized^{1,2)}. However, there are other measures of smoothness to be considered by the designers.

In this study, a new approach is proposed for shape optimization of shells modeled using Bézier surface. The strain energy is used to represent the mechanical performance, and the aesthetic aspects and smoothness of the surface are quantified by algebraic invariants of the surface representing curvature, convexity, gradient, etc. The condition of the developable surface is ensured by incorporating the constraints on the principal curvature.

2. Shape representation by Bézier surface

The number of variables for optimization can be drastically reduced without sacrificing smoothness and complexity of the surface using the Bézier surface. Moreover, the basis functions of Bézier surface can be expressed explicitly with respect to the coordinates of the control points, which enables us to carry out sensitivity analysis of the algebraic invariants analytically.

2.1. Tensor product Bézier surface

The point $S_{I,J}(s, t) = [x(s, t), y(s, t), z(s, t)]^T$ on a tensor product Bézier surface is defined with parameters $s, t \in [0, 1]$ as

$$S_{I,J}(s, t) = \sum_{i=0}^I \sum_{j=0}^J q_{ij} B_{I,i}(s) B_{J,j}(t) \quad (1)$$

where $q_{ij} = [q_{x,ij}, q_{y,ij}, q_{z,ij}]^T$ is the control point, and $B_{I,i}(s)$ and $B_{J,j}(t)$ are the Bernstein basis functions. I and J are the orders of the functions. The vectors of x -, y -, and z -coordinates of control points are denoted by q_x , q_y , and q_z , respectively; e.g., q_x is defined as

$$q_x = [q_{x,00}, \dots, q_{x,0J}, \dots, q_{x,I0}, \dots, q_{x,IJ}]^T \quad (2)$$

2.2. Triangular patch Bézier surface

The point $S_n(u, v, w) = [x(u, v, w), y(u, v, w), z(u, v, w)]^T$ on a triangular patch Bézier surface is defined with parameters $u, v, w \in [0, 1](u + v + w = 1)$ as

$$S_n(u, v, w) = \sum_{i+j+k=n} q_{ijk} B_{n,ijk}(u, v, w) \quad (i, j, k = 0, 1, \dots, n, \quad 0^0 = 0! = 1) \quad (3)$$

where $q_{ijk} = [q_{x,ijk}, q_{y,ijk}, q_{z,ijk}]^T$ is the control point, $B_{n,ijk}(u, v, w)$ is the bivariate Bernstein basis function, and n is the order of the function. The vectors of x -, y -, and z -coordinates of control points are denoted by q_x , q_y , and q_z , respectively; e.g., q_x is defined as

$$q_x = [q_{x,00I}, \dots, q_{x,I00}, q_{x,01I-1}, \dots, q_{x,I-110}, \dots, q_{x,0I0}]^T \quad (4)$$

3. β invariants and γ invariants

We use the six algebraic invariants $\beta_0, \beta_1, \beta_2, \gamma_1, \gamma_2,$ and γ_3 proposed by Iri *et al.*³⁾ for representing the geographical properties. Here, we regard z -coordinates of the Bézier surface as the altitude of the geographical representation.

3.1. Definitions of tensors and vectors

Here, only the invariants on the tensor product Bézier surface is formulated. In the following, the covariant and the contravariant components are indicated by the subscript and superscript, respectively. The components of the covariant gradient vector \underline{z} , the covariant hessian \underline{h} , and the covariant metric tensor \underline{g} are defined

$$\underline{z} = \begin{bmatrix} z_s \\ z_t \end{bmatrix}, \quad \underline{h} = \begin{bmatrix} h_{ss} & h_{st} \\ h_{ts} & h_{tt} \end{bmatrix}, \quad \underline{g} = \begin{bmatrix} g_{ss} & g_{st} \\ g_{ts} & g_{tt} \end{bmatrix} \quad (5)$$

which are obtained from

$$z_s = \frac{\partial z(s, t)}{\partial s}, \quad z_t = \frac{\partial z(s, t)}{\partial t} \quad (6)$$

$$h_{ss} = \frac{\partial^2 z(s, t)}{\partial s^2}, \quad h_{tt} = \frac{\partial^2 z(s, t)}{\partial t^2}, \quad h_{st} = h_{ts} = \frac{\partial^2 z(s, t)}{\partial s \partial t} \quad (7)$$

$$g_{ss} = \frac{\partial \mathbf{S}_{I,J}(s, t)^\top}{\partial s} \frac{\partial \mathbf{S}_{I,J}(s, t)}{\partial s}, \quad g_{tt} = \frac{\partial \mathbf{S}_{I,J}(s, t)^\top}{\partial t} \frac{\partial \mathbf{S}_{I,J}(s, t)}{\partial t} \quad (8)$$

$$g_{st} = g_{ts} = \frac{\partial \mathbf{S}_{I,J}(s, t)^\top}{\partial s} \frac{\partial \mathbf{S}_{I,J}(s, t)}{\partial t}$$

Let \bar{z} and \bar{g} denote the contravariant gradient vector of z -coordinate and the contravariant metric tensor, respectively. Then the following relations holds:

$$\bar{g} = \underline{g}^{-1}, \quad \bar{z} = \bar{g}\underline{z}, \quad \underline{z} = \underline{g}\bar{z} \quad (9)$$

In addition, we define the following contravariant vector \tilde{z} :

$$\tilde{z} = \begin{bmatrix} \tilde{z}^s \\ \tilde{z}^t \end{bmatrix} = \tilde{\mathbf{E}}\underline{z}, \quad \tilde{\mathbf{E}} = \begin{bmatrix} \tilde{E}^{11} & \tilde{E}^{12} \\ \tilde{E}^{21} & \tilde{E}^{22} \end{bmatrix} = \begin{bmatrix} 0 & 1 \\ -1 & 0 \end{bmatrix} \quad (10)$$

The product of a covariant vector and a contravariant vector, and the bilinear form with respect to a second-order covariant/contravariant tensor and a contravariant/covariant vector are invariant with respect to the definition of the parameter of the surface. Then, β and γ invariants are defined as follows:

$$\beta_0 = \sum_{\xi=s,t} \sum_{\lambda=s,t} g^{\xi\lambda} z_\xi z_\lambda = \sum_{\xi=s,t} z^\xi z_\xi (\geq 0) \quad (11)$$

$$\beta_1 = \sum_{\xi=s,t} \sum_{\lambda=s,t} h_{\lambda\xi} g^{\xi\lambda} \quad (12)$$

$$\beta_2 = \frac{1}{2\det(\underline{g})} \sum_{\xi=s,t} \sum_{\lambda=s,t} \sum_{\mu=s,t} \sum_{\nu=s,t} h_{\nu\lambda} h_{\mu\xi} \tilde{E}^{\xi\lambda} \tilde{E}^{\mu\nu} \quad (13)$$

$$\gamma_1 = \sum_{\lambda=s,t} \sum_{\xi=s,t} h_{\lambda\xi} \tilde{z}^{\xi} \tilde{z}^{\lambda} \quad (14)$$

$$\gamma_2 = \sum_{\lambda=s,t} \sum_{\xi=s,t} h_{\lambda\xi} \tilde{z}^{\xi} \tilde{z}^{\lambda} = \sum_{\lambda=s,t} \sum_{\xi=s,t} h_{\lambda\xi} \tilde{z}^{\xi} \tilde{z}^{\lambda} \quad (15)$$

$$\gamma_3 = \frac{1}{\det(\underline{g})} \sum_{\lambda=s,t} \sum_{\xi=s,t} h_{\lambda\xi} \tilde{z}^{\xi} \tilde{z}^{\lambda} \quad (16)$$

For the triangular patch Bézier surface, We only have to replace s, t with u, v (w), and I, J with n , respectively. Note that w is automatically assigned from u and v using $w = 1 - u - v$.

4. Surface properties based on algebraic invariants

The six algebraic invariants $\beta_0, \beta_1, \beta_2, \gamma_1, \gamma_2$, and γ_3 , defined using the vectors and tensors given in Sec.3. 1., are used for quantitative evaluation of the surface properties. The local properties in the neighborhood of a point P on the surface are characterized by the invariants as follows:

$\beta_2 > 0$ The contours in the neighbourhood of P are coaxial (part of) similar ellipses. Especially, when $\beta_1^2 = 4\beta_2$, the contours are (part of) concentric circles and the surface is locally isotropically curved. The shape is locally concave if $\beta_1 > 0$, and locally convex if $\beta_1 < 0$.

$\beta_2 < 0$ The contours in the neighbourhood of P are (part of) coaxial hyperbolas. Locally, the surface is convex in some directions and concave in others. There are special directions in which the contour lines are straight (i.e., neither concave nor convex).

$\beta_2 = 0$ One of the principal curvatures is 0. Furthermore, the other principal curvature is positive if $\beta_1 > 0$; and negative if $\beta_1 < 0$; and 0 if $\beta_1 = 0$ that means a locally flat surface.

$\beta_0 = 0$ P is a critical point (locally maximum/minimum value of z -coordinate).

$\gamma_2 = 0$ Direction of gradient vector coincides with one of the principal direction, and the surface near P is locally cylindrical and concave in one principal direction if $|\gamma_1| < |\gamma_3|$ and $\gamma_3 > 0$; whereas it is locally cylindrical and convex in one principal direction if $|\gamma_1| < |\gamma_3|$ and $\gamma_3 < 0$.

In addition, β_1 and β_2 correspond to the twice the average curvature and the Gaussian curvature, respectively. Furthermore, γ_1/β_0 is the curvature in the steepest descent direction, and γ_3/β_0 is the curvature in its perpendicular direction.

In view of constructability, it is desirable that the surface can be developed to a plane without expansion or contraction. Such surface is called developable surface, which is characterized

by vanishing Gaussian curvature. Therefore, to generate a developable surface, the constraint $\beta_2 = 0$ should be satisfied at any point on the surface.

5. Numerical examples

5.1. Description of shell model and optimization problem

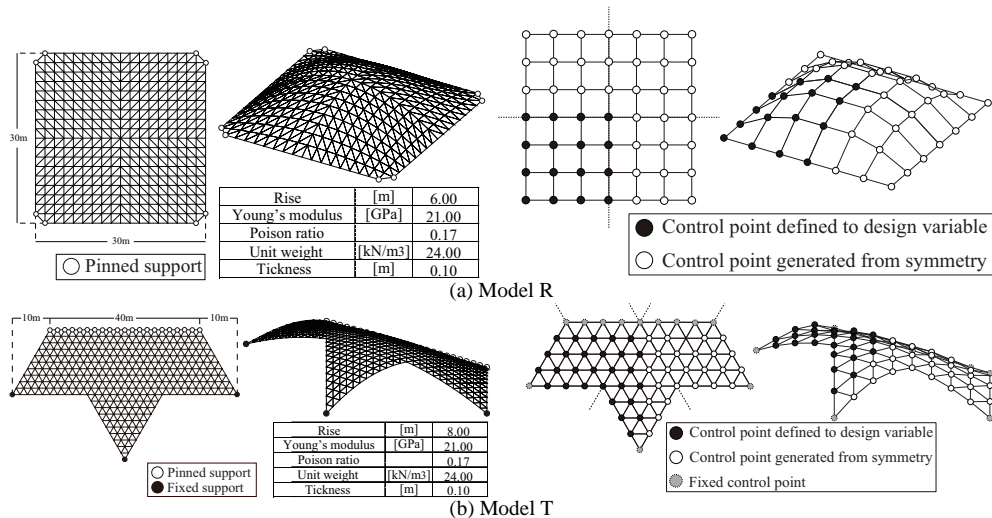


Figure 1 : Plan, diagonal view, various parameter values, and Bézier patches of rectangular and triangular models

The shapes of the shell structures shown in Figure 1 are optimized considering the algebraic invariants and the strain energy under self-weight. Displacements and stresses under self-weight are calculated by linear static finite element analysis. The constant strain triangular element⁴⁾ is adopted for the in-plane deformation and nonconforming triangle element proposed by Zienkiewics *et al.*⁵⁾ is adopted for the out-of-plane deformation. The design variables of each model are the z -coordinates q_z of the control points which are reduced using symmetry conditions. For model T, the control points on the fixed supports are excluded from the design variable. The continuity of the gradient and curvature along the interior boundary between Bézier patches is not necessarily satisfied.

The optimum shape is found under constraints on the coordinates of the model R's supports and the algebraic invariants. Moreover, to prevent unrealistic shape with extremely large rise, and to improve the convergence property of optimization algorithm, an upper bound is given for the area of shell's middle surface (henceforth area). Since the shell has a uniform thickness, the area constraint is equivalent to the volume or weight constraint that is usually regarded as representing the material cost.

In each of the optimization problem formulated below, total number of degrees of freedom, nodal displacement vector, linear stiffness matrix, area, and vector consisting of z -coordinates

of the Model R's supports are denoted by n , $\mathbf{d} \in R^n$, $\mathbf{K} \in R^{n \times n}$, S , and $\mathbf{r}_z^* \in R^2$, respectively. The value of the initial shape is shown by 0 subscript. The sequential quadratic programming method in SNOPT⁽⁶⁾ is used for optimization.

5. 2. Optimal solutions of model R

5. 2. 1. Optimal shape without constraints on algebraic invariants

We first find optimal shape without constraints on algebraic invariants. The strain energy is minimized as follows under constraints on the locations of the supports, and the upper-bound constraint on the area:

$$\begin{aligned} & \text{minimize} && f(\mathbf{q}_z) = \frac{1}{2} \mathbf{d}^T \mathbf{K} \mathbf{d} \\ & \text{subject to} && \begin{cases} S - S_0 \leq 0 \\ \mathbf{r}_z^* - \mathbf{r}_{z,0}^* = 0 \end{cases} \end{aligned} \quad (17)$$

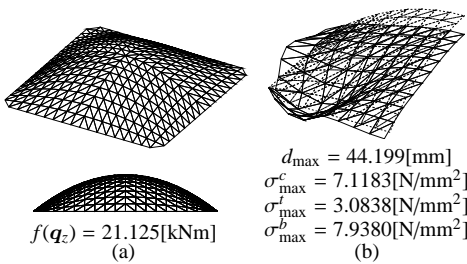


Figure 2 : Initial shape

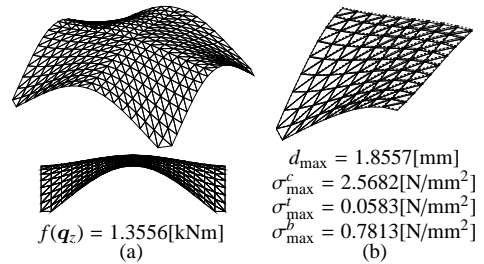


Figure 3 : Optimal shape

The initial and optimal shapes are shown in Figures 2(a) and 3(a), respectively. The dashed and solid lines, respectively, in Figures 2(b) and 3(b) are the undeformed and deformed shapes, where the displacements are magnified by the factor 100. The optimal objective value $f(\mathbf{q}_z)$, maximum values of displacement d_{\max} , compressive stress σ_{\max}^c , tensile stress σ_{\max}^t , and bending stress σ_{\max}^b are also shown in the figures. It can be confirmed from the optimization result that bending and tensile stresses are reduced and the shape is optimized so that the shell resists the self-weight mainly with compression.

5. 2. 2. Optimal shape with constraints on β invariants

We next consider the following optimization problem by introducing the constraints on β invariants to obtain a locally convex surface:

$$\begin{aligned} & \text{minimize} && f(\mathbf{q}_z) = \frac{1}{2} \mathbf{d}^T \mathbf{K} \mathbf{d} \\ & \text{subject to} && \begin{cases} S - S_0 \leq 0 \\ \mathbf{r}_z^* - \mathbf{r}_{z,0}^* = 0 \\ \beta_2^c > 0 \\ \beta_1^c \leq \bar{\beta} \end{cases} \end{aligned} \quad (18)$$

● β constraint point

c : Invariants constraints point

where $\bar{\beta} < 0$ to ensure convexity around point c indicated by the dot in the figure.

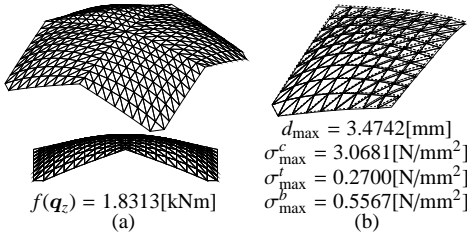


Figure 4 : Optimal shape ($\bar{\beta} = -0.1$)

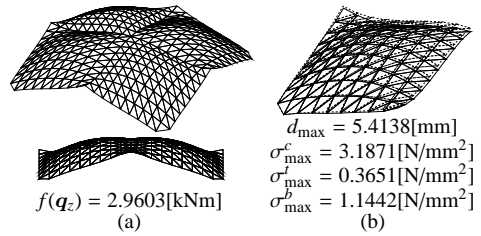


Figure 5 : Optimal shape ($\bar{\beta} = -0.15$)

Figures 4 and 5 show the optimization results for $\bar{\beta} = -0.1$ and -0.15 , respectively. As is seen, the maximum values of displacement, compressive stress, and tensile stress increase as a result of assigning requirement of local convexity. The displacement and stresses also increase by increasing the absolute value of β_1^c .

5. 2. 3. Optimal shape with constraints on γ invariants

We next solve the following problem with constraints on γ invariants to obtain locally cylindrical and convex surface:

$$\begin{aligned}
 &\text{minimize } f(\mathbf{q}_c) = \frac{1}{2} \mathbf{d}^T \mathbf{K} \mathbf{d} \\
 &\text{subject to } \begin{cases} S - \bar{S}_0 \leq 0 \\ \mathbf{r}_z^* - \mathbf{r}_{z,0}^* = 0 \\ \gamma_2^{ci} = 0 \\ \gamma_3^{ci2} - \gamma_1^{ci2} > 0 \\ \gamma_3^{ci} \leq \bar{\gamma}^{ci} \end{cases} \quad \begin{matrix} \text{● } \gamma \text{ constraint points} \\ \text{ci : Invariants constraints point} \end{matrix} \quad (19)
 \end{aligned}$$

where the constraints on the γ invariants are given at points $c1$ and $c2$ indicated by dots in the figure.

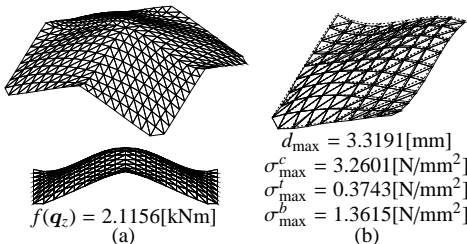


Figure 6 : Optimal shape ($\bar{\gamma}^i = -0.015$)

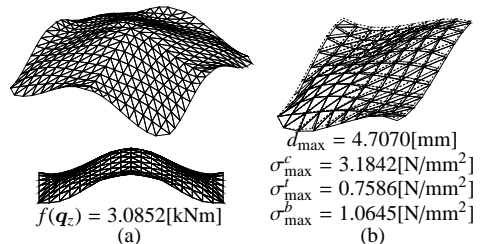


Figure 7 : Optimal shape ($\bar{\gamma}^i = -0.025$)

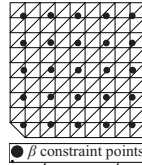
Figures 6 and 7 show the optimization results for $\bar{\gamma}^{c1} = \bar{\gamma}^{c2} = -0.015$ and $\bar{\gamma}^{c1} = \bar{\gamma}^{c2} = -0.025$, respectively. It can be confirmed that a locally cylindrical and convex surface has

been successfully obtained by introducing the constraints on the γ invariants.

5. 2. 4. Optimal shape with developability constraints

Finally, we generate a developable surface by shape optimization. The following problem is to be solved so that β_2 vanishes at 25 points indicated by the dots in the figure:

$$\begin{aligned} & \text{minimize} && f(\mathbf{q}) = \frac{1}{2} \mathbf{d}^T \mathbf{K} \mathbf{d} \\ & \text{subject to} && \begin{cases} S - S_0 \leq 0 \\ \mathbf{r}_{z,0}^* - \mathbf{r}_{z,0} = 0 \\ \beta_2^{ci} = 0 \\ (i=1, \dots, 25) \end{cases} \end{aligned} \quad (20)$$



ci : Invariants constraints point

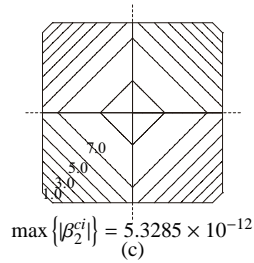
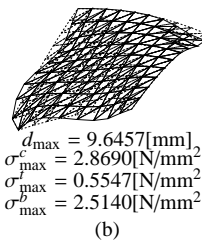
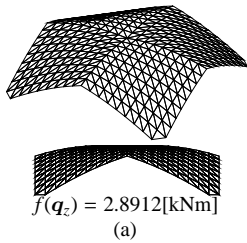


Figure 8 : Optimal shape

The optimal shape is shown in Figure 8. It can be seen from Figure 8(c) that maximum value of β_2^{ci} has been successfully minimized, although there is no guarantee that β_2 becomes 0 at the points where the constraints are not given. The contour lines became almost straight and parallel. It can be confirmed from Figure 8(a) 1/4 part of model R seems to be developable. Furthermore, both of the strain energy and the maximum vertical displacement have smaller values than the initial shape.

5. 3. Optimal solutions of model T

5. 3. 1. Optimal shape without constraints on algebraic invariants

We first find optimal shape without constraints on algebraic invariants. The strain energy is minimized as follows under constraints on the upper-bound constraint on the area:

$$\begin{aligned} & \text{minimize} && f(\mathbf{q}_z) = \frac{1}{2} \mathbf{d}^T \mathbf{K} \mathbf{d} \\ & \text{subject to} && S - S_0 \leq 0 \end{aligned} \quad (21)$$

The initial and optimal shapes are shown in Figures 9(a) and 10(a), respectively. The dashed and solid lines, respectively, in Figures 9(b) and 10(b) are the undeformed and deformed shapes, where the displacements are magnified by the factor 50. Like a model R, it can be confirmed from the optimization result that bending and tensile stresses are reduced and the shape is optimized so that the shell resists the self-weight mainly with compression.

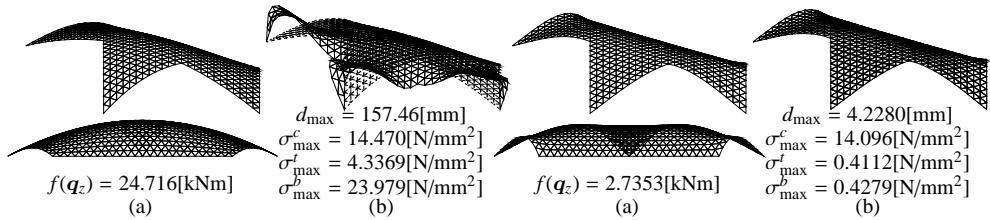


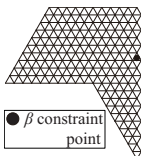
Figure 9 : Initial shape

Figure 10 : Optimal shape

5.3.2. Optimal shape with constraints on β invariants

We next consider the following optimization problem by introducing the constraints on β invariants to obtain a locally convex surface:

$$\begin{aligned}
 &\text{minimize} && f(\mathbf{q}_z) = \frac{1}{2} \mathbf{d}^T \mathbf{K} \mathbf{d} \\
 &\text{subject to} && \begin{cases} S - S_0 \leq 0 \\ \beta_2^c > 0 \\ \beta_1^c \leq \bar{\beta} \end{cases}
 \end{aligned}
 \tag{22}$$



β_2^c : β_2 value at point c
 β_1^c : β_1 value at point c

c : Invariants constraints point

where $\bar{\beta} < 0$ to ensure convexity around point c indicated by the dot in the figure.

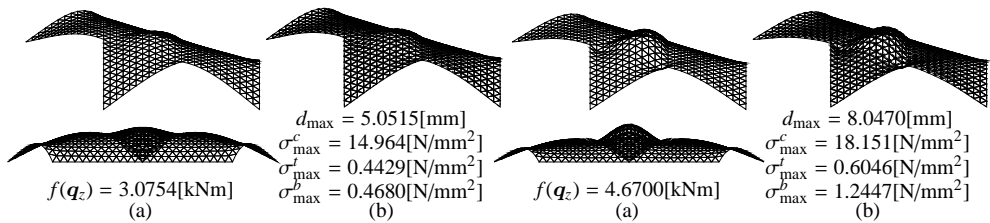


Figure 11 : Optimal shape ($\bar{\beta} = -0.2$)

Figure 12 : Optimal shape ($\bar{\beta} = -0.4$)

Figures 11 and 12 show the optimization results for $\bar{\beta} = -0.2$ and -0.4 , respectively. As is seen, the maximum values of displacement, compressive stress, and tensile stress increase as a result of assigning requirement of local convexity. The displacement and stresses also increase by increasing the absolute value of β_1^c .

5.3.3. Optimal shape with constraints on γ invariants

We next solve the following problem with constraints on γ invariants to obtain locally cylindrical and convex surface:

$$\begin{aligned} & \text{minimize } f(\mathbf{q}_z) = \frac{1}{2} \mathbf{d}^T \mathbf{K} \mathbf{d} \\ & \text{subject to } \begin{cases} S - S_0 \leq 0 \\ \gamma_2^{ci} = 0 \\ \gamma_3^{ci2} - \gamma_1^{ci2} > 0 \\ \gamma_3^{ci} \leq \bar{\gamma}^{ci} \\ (i=1, \dots, 4) \end{cases} \end{aligned} \quad \begin{array}{l} \text{● } \gamma \text{ constraint} \\ \text{points} \\ \gamma_2^{ci} : \gamma_2 \text{ value at point } ci \\ \gamma_1^{ci} : \gamma_1 \text{ value at point } ci \end{array} \quad (23)$$

ci : Invariants constraints point

where the constraints on the γ invariants are given at points ci ($i = 1, \dots, 4$) indicated by dots in the figure.

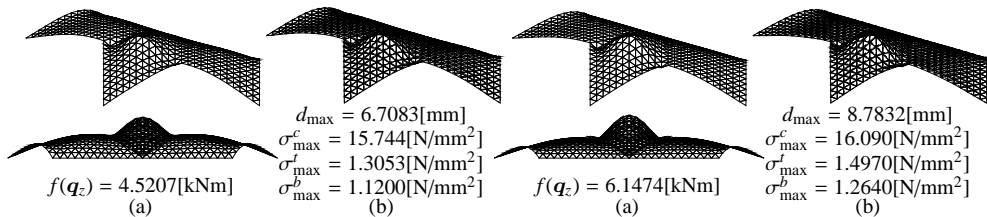


Figure 13 : Optimal shape ($\bar{\gamma} = -0.03$)

Figure 14 : Optimal shape ($\bar{\gamma} = -0.05$)

Figures 13 and 14 show the optimization results for $\bar{\gamma}^{ci} = -0.03$ and $\bar{\gamma}^{ci} = -0.05$, respectively ($i = 1, \dots, 4$). It can be confirmed that a locally cylindrical and convex surface has been successfully obtained by introducing the constraints on the γ invariants.

5.3.4. Optimal shape with developability constraints

Finally, we generate a developable surface by shape optimization. The following problem is to be solved so that β_2 vanishes at 25 points indicated by the dots in the figure:

$$\begin{aligned} & \text{minimize } f(\mathbf{q}) = \frac{1}{2} \mathbf{d}^T \mathbf{K} \mathbf{d} \\ & \text{subject to } \begin{cases} S - S_0 \leq 0 \\ \beta_2^{ci} = 0 \\ (i=1, \dots, 20) \end{cases} \end{aligned} \quad \begin{array}{l} \text{● } \beta \text{ constraint} \\ \text{points} \\ \beta_2^{ci} : \beta_2 \text{ value at point } ci \end{array} \quad (24)$$

ci : Invariants constraints point

The optimal shape is shown in Figure 15. It can be seen from Figure 15(c) that maximum value of β_2^{ci} has been successfully minimized, although there is no guarantee that β_2 becomes 0 at the points where the constraints are not given. The contour lines became almost straight and parallel. According to the contour lines of Figures 15(d), 1/6 part of model T seems to be nearly developable. Furthermore, both of the strain energy and the maximum vertical displacement have smaller values than the initial shape.

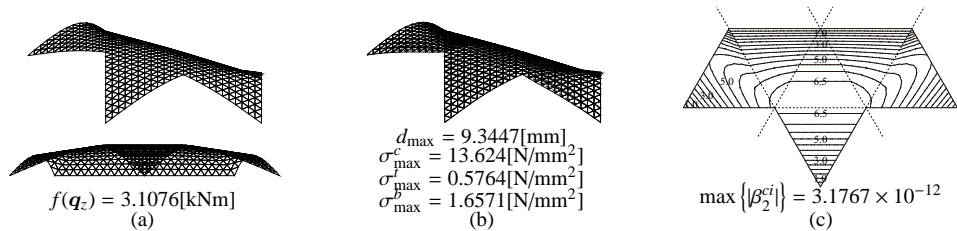


Figure 15 : Optimal shape

6. Conclusions

The local properties of the shell surface can be explicitly controlled by solving an optimization problem with constraints on the algebraic invariants of the surface. Moreover, a developable surface can be obtained by assigning the constraint such that the Gaussian curvature vanishes everywhere on the surface. It is showed from the analytical result in various models which is modeled by tensor product Bézier surface and triangular patch Bézier surface that this method can apply to the shell that has various flat types and boundary conditions widely. It may be concluded that the algebraic invariants are effective indices representing the local properties of the surface, and the optimal shell shape considering the aesthetic aspects, constructability and mechanical rationality can be generated using the proposed approach at the early design stage.

References

- [1] M. Ohsaki and M. Hayashi, Fairness metrics for shape optimization of ribbed shells, *J. Int. Assoc. Shells and Spatial Struct.*, 2000, Vol. 41(1), pp. 31–39
- [2] M. Ohsaki, T. Ogawa and R. Tateishi, Shape optimization of curves and surfaces considering fairness metrics and elastic stiffness, *Struct. Multidisc. Optim.*, 2003, Vol. 24, pp. 449–456, Erratum: 2004, Vol. 27, pp. 250–258
- [3] M. Iri, Y. Shimakawa, and T. Nagai, Extraction of invariants from digital elevation data with application to terrain topography, *Nonlinear Analysis*, 2001, Vol.47, pp. 5585–5598
- [4] S. Timoshenko, and K. Woinowsky, *Theory of plates and shells*, McGraw-Hill, 1959
- [5] G. P. Bazeley, Y. K. Cheung, B. M. Irons, and O. C. Zienkiewicz, Triangular elements in bending–conforming and nonconforming solutions, *Proceedings of the Conference on Matrix Methods in Structural Mechanics*, 1959, pp.547–576
- [6] P. Gill, W. Murray, and M. Saunders, *User’s Guide for snopt Version 7 : Software for Large-Scale Nonlinear Programming*, Stanford Business Software Inc., 2008